ECS Transactions, 25 (8) 161-171 (2009)
10.1149/1.3207587 ©The Electrochemical Society

Mechanism-Based Design of Precursors for MOCVD

Lisa McElwee-White,[a,*] Jürgen Koller,[a] Dojun Kim,[b] and Timothy J. Anderson[b]

[a] Department of Chemistry, University of Florida, Gainesville, Florida 32611 USA
[b] Department of Chemical Engineering, University of Florida, Gainesville, Florida 32611 USA

A chemistry-based approach to designing precursors for the deposition of inorganic films requires consideration of the physical properties of the precursor compound (*e.g.*, volatility for transport in the reactor) and its probable decomposition pathways, both in the gas phase and on the surface during growth. We have been using Aerosol-Assisted Chemical Vapor Deposition of tungsten carbonitride (WN_xC_y) films from tungsten imido complexes and tungsten hydrazido complexes as a model system to investigate the relationship between data obtained from conventional organometallic mechanistic study of the precursors and the resulting film deposition kinetics and film properties. Among the typical techniques for the elucidation of decomposition pathways in organometallic compounds that will be discussed in this context are NMR kinetics, mass spectrometry, DFT calculations, and single crystal X-ray diffractometry.

Introduction

Deposition of thin films of inorganic materials has been of great recent interest, in part due to technological applications in the electronics industry. The surface reactions that result in film formation during chemical vapor deposition (CVD) and the related technique atomic layer deposition (ALD) provide opportunities for growth of highly conformal thin layers of material on patterned substrates, an advantage of chemical deposition methods as compared to physical deposition methods such as sputtering. Careful choice of reaction chemistry could also be used to control composition and properties of the resulting films (1). These considerations have led to recent efforts to design precursors using chemical strategies (2-8).

Our approach to precursor design is a mechanism-based strategy in which known pathways for thermal decomposition of organometallic complexes have been used to predict the reactivity of precursors during CVD. The challenge is the difference between reaction conditions used in the majority of mechanistic studies (complexes in solution at or below room temperature) and the conditions used in CVD (gas/surface reaction at temperatures ≥ 300 °C). Under CVD conditions, not only are the typical solution-phase organometallic reaction pathways faster but new reaction manifolds can become accessible (9). An additional challenge in precursor design is the need to transport the precursor to the substrate surface in the vapor phase. In the case of conventional CVD reactors that utilize bubblers or sublimators for volatilization of the precursor, attention to the relationship between molecular structure and the volatility of the complexes is required.

Because of the importance of transition metal nitrides as diffusion barrier materials to prevent migration of Al or Cu metallization into the Si device layer or the dielectric layers of integrated circuits (7), we have chosen deposition of metal nitride and the related carbonitride films for testing of our design strategies. We have recently been using Aerosol-Assisted Chemical Vapor Deposition (AACVD) of tungsten carbonitride (WN_xC_y) films from the tungsten imido complexes $WCl_4(NR)(CH_3CN)$ [**1**: R = Ph; **2**: R = ^{i}Pr; **3**: R = allyl] (10-12) and the tungsten hydrazido complexes $WCl_4(NNR_2)(CH_3CN)$ [**4**: R_2 = Me_2; **5**: Ph_2; **6**: R = -$(CH_2)_5$-] (13, 14) as a model system to investigate the relationship between data obtained from conventional organometallic mechanistic study and the resulting film deposition kinetics and film properties.

Among the standard techniques for the elucidation of decomposition pathways in organometallic compounds that we have applied in this context are NMR kinetics, mass spectrometry, DFT calculations, and small molecule structure determination by single crystal X-ray diffractometry. Information on the precursor chemistry found through these means can be correlated to film composition (AES, XRD), film growth kinetics (X-SEM), bonding in the films (XPS), and electrical resistivity (four-point probe). Selected examples will be discussed below.

Results and Discussion

Precursor design. Our choice of the tungsten imido complexes $WCl_4(NR)(CH_3CN)$ (**1**-**3**) and the tungsten hydrazido complexes $WCl_4(NNR_2)(CH_3CN)$ (**4**-**6**) as precursors

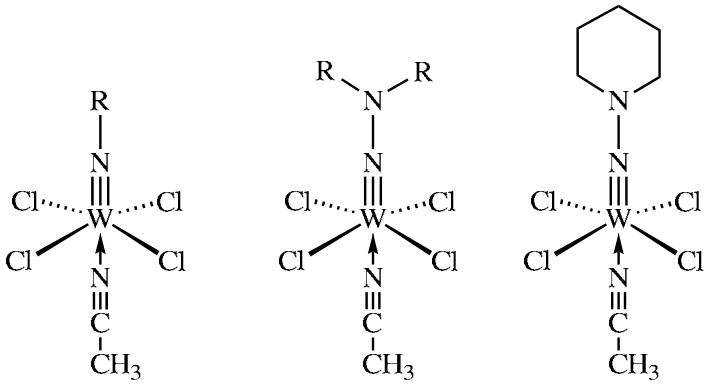

1 R = Ph
2 R = ^{i}Pr
3 R = allyl

4 R = Me
5 R = Ph

6

Figure 1. Structures of precursors **1-6**.

for the deposition of WN_xC_y films shares some common features with the selection of the dimeric complexes $[MCl_2(N^tBu)(NH^tBu)(NH_2{}^tBu)]_2$ (M = Nb, Ta) (15) as CVD precursors for films of NbN and Ta_3N_5, respectively, and the use of $TiCl_2(N^tBu)(py)_3$ to deposit TiN (16, 17). All of these precursors contain combinations of an imido group, chlorides and other N-bound ligands (amines, amides and nitriles). In each case, the imido ligand provides a strong M-N multiple bond, which is likely to survive decomposition of the complex during deposition and provide a building block for the

assembly of metal nitrides on the substrate surface. In our complexes **1-6**, the strong *trans* effect of the imido or hydrazido ligand is expected to facilitate dissociation of the nitrile ligand, which is *trans* to the imido or hydrazido moiety in all of these compounds. Our synthetic routes to complexes **1-6** allow for considerable flexibility in the imido and hydrazido substituents, which in turn allows manipulation of bond dissociation energies within those moieties. During film deposition, the chloride ligands are removed from precursors **1-6** as HCl by addition of H_2 or NH_3 to the carrier gas (9, 18-20). Although the imido and hydrazido complexes **1-6** are non-volatile solids, they can be volatilized for AACVD by nebulizing a solution of the precursor in benzonitrile (11).

Experimental Results

Mass Spectrometry. In evaluating our precursor designs and screening precursors before deposition experiments, we utilize the correlation between mass spectrometric fragmentation patterns and likely decomposition pathways during deposition (21, 22). Since mass spectrometry involves gas phase ions while CVD is a heterogeneous thermal process, over-interpretation should be avoided but we have found that fragmentation patterns can be useful qualitative predictors of CVD behavior. As an example, the mass spectra of the series $WCl_4(NR)(CH_3CN)$ (**1-3**) exhibit significant differences that are reflected in the behavior of the complexes during CVD.

TABLE I. Summary of relative abundances for negative ion (NCI) mass spectra of imido complexes **1-3**.

Complex	NCI Fragments	*m/z*	Abundance	Reference
1	$[WCl_4(NPh)]^-$	417	100	(10)
	$[WCl_4N]^-$	340	4	(10)
2	$[WCl_4(N^iPr)]^-$	383	42	(11)
	$[WCl_4N]^-$	340	100	(11)
3	$[WCl_4(NC_3H_5)]^-$	381	5	(12)
	$[WCl_4N]^-$	340	100	(12)

One critical piece of information involves the facility of N-C bond cleavage in the imido moiety. The tendency for cleavage of the N(imido)-C bond can be discerned in the negative ion chemical ionization mass spectrometry (NCI-MS) data for **1-3** (Table 1) through the abundance of the $[WCl_4N]^-$ ion, in which the alkyl substituent has already dissociated to leave a tungsten nitrido fragment. For complexes **2** (R = ^{i}Pr) and **3** (R = allyl) this nitrido ion gives rise to the base peak of the NCI mass spectrum. The behavior of the phenylimido complex **1** is very different in that the $[WCl_4N]^-$ fragment exhibits only 4% of the integrated intensity of the mass envelope for its base peak $[WCl_4(NPh)]^-$. These data suggest difficulty in cleavage of the N-C(imido) bond of phenylimido complex **1**, which will result in corresponding problems with growth of WN_xC_y. Further insight can be gained from examination of the positive ion EI spectrum of **1**, in which observation of $[WCl_4]^+$ and $[WCl_3]^+$ fragments implies preferential cleavage of the W-N bond instead of cleavage of the N-C(imido) bond (11). W-N cleavage results in loss of the intact NPh ligand during film growth and thus low N levels in the resulting films. This qualitative information on trends for preferred bond cleavage in the imido complexes **1-3** is consistent with the nitrogen content of films grown from the three precursors. For low temperature film growth, precursors which exhibit facile N-C bond dissociation in the NCI-MS (**2** and **3**) afford films with higher nitrogen levels than those grown from **1**, in which W-N dissociation competes well with N-C dissociation during precursor decomposition (Figure 2).

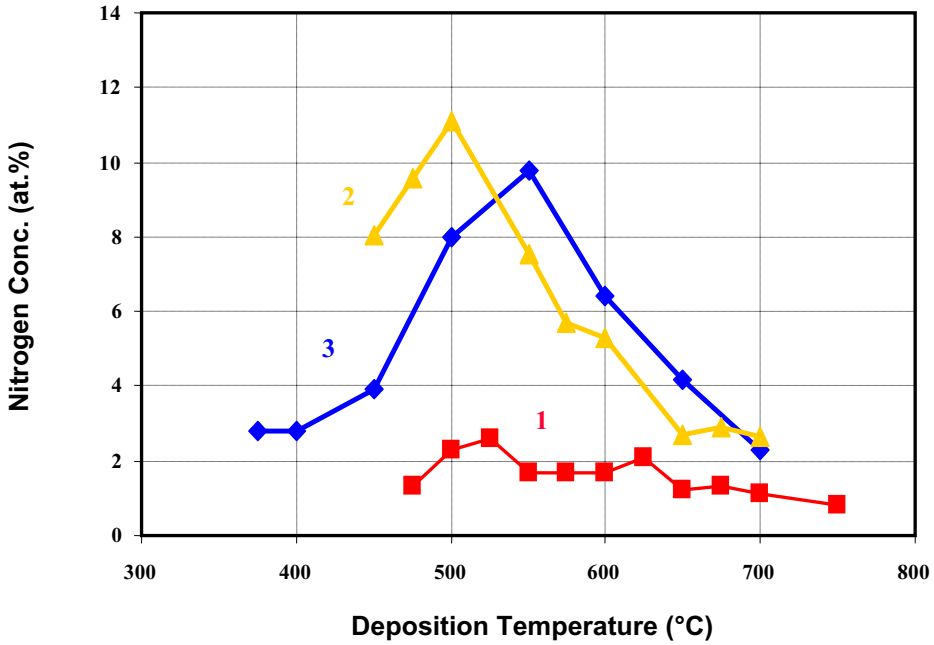

Figure 2. Comparison of nitrogen content in the films grown from **1-3**. Figure reproduced with permission from reference (9). Copyright 2006, American Chemical Society.

Information from the mass spectra can also be correlated to changes in the apparent activation energies for film growth from precursors **1-3**. The integrated intensities of the peaks for the $[WCl_4N]^-$ ion rise as the imido substituent changes from phenyl to isopropyl to allyl (**1** → **2** → **3**). There is a parallel decrease in the bond dissociation energy (BDE) of the N−C bond in the imido moiety, as modeled by N-C BDEs of the corresponding primary amines RNH_2. From the amine data, the N−C bond of allylimido complex **3** should be approximately 11 kcal/mol weaker than that of isopropylimido complex **2** and 32 kcal/mol weaker than that of phenylimido complex **1** (23). The relative magnitudes of the apparent activation energy E_a for film deposition from **1-3** follow a trend that is consistent with both the intensity of the $[WCl_4N]^-$ ion in the mass spectra and with the strength of the imido N−C bond, as predicted from the organic model compounds. The linear relationship between the estimated N-C BDE and E_a (Figure 3) is consistent with cleavage of the N−C imido bond before or during the rate-determining step for film growth. Thus, the strength of the N-C bond in the imido moiety is critical in two regards: 1) partitioning between W-N and N-C cleavage, which affects the film composition and 2) determination of the apparent activation energy, which determines the rate of film growth. This type of information can then be used in design of additional precursors.

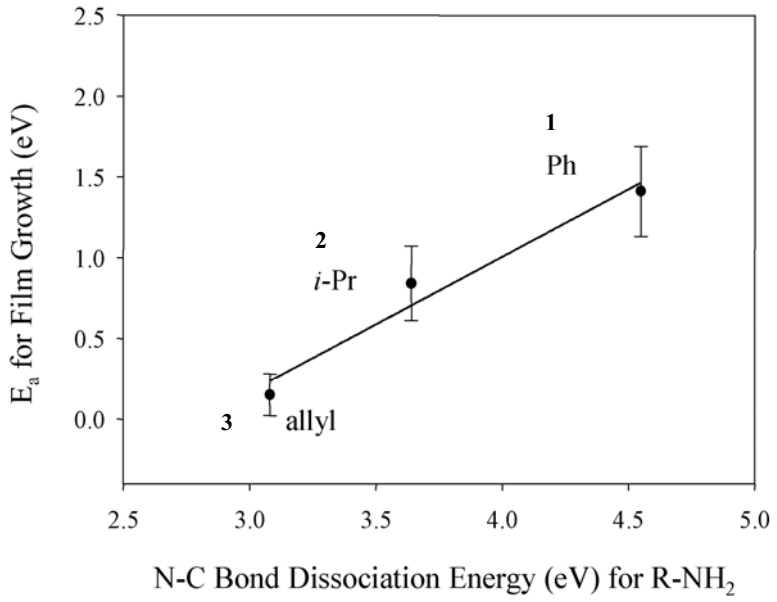

Figure 3. Variation of apparent activation energy (E_a) for film growth from **1-3** with the N−C bond energies of the corresponding amines R-NH_2 as models for the imido N-C bonds. Figure reproduced with permission from reference (12). Copyright 2005, American Chemical Society.

NMR kinetics. One of the design features of precursors **1-6** was a facile initial dissociation of the CH_3CN ligand during film growth, which was postulated on the basis of the strong *trans* effect of the imido/hydrazido ligand in the dissociative reactions of imido complexes (24). This reaction pathway is consistent with the mass spectra of **1-3**, in which molecular ions cannot be observed and the highest *m/z* values in both positive and negative modes correspond to ions from which CH_3CN has been lost (10-12).

To obtain experimental values for the activation energy of CH_3CN dissociation, complex **2** was chosen as a representative case. ^{1}H NMR kinetics were used to study the exchange of the acetonitrile ligand of **2** with free CH_3CN in $CDCl_3$ solution. Both bound and free acetonitrile could be detected in the ^{1}H NMR spectra obtained at -20˚C and the two signals coalesced with increasing temperature. The exchange rate k for the exchange of acetonitrile was determined by line-shape analysis in the temperature range -6 to 34 °C. The activation energy of 18.52 ± 0.14 kcal/mol and an entropy of activation of 15.8 ± 0.5 cal/mol•K were obtained from a plot of ln(k/T) vs. 1/T (Figure 4) and correspond to $\Delta H^{\ddagger}$ and $\Delta S^{\ddagger}$ for dissociative loss of CH_3CN from isopropylimido complex **2**. Since this process can be easily followed at 34 °C, loss of acetonitrile from **1-6** must be kinetically facile under CVD conditions, which involve temperatures above 300 °C.

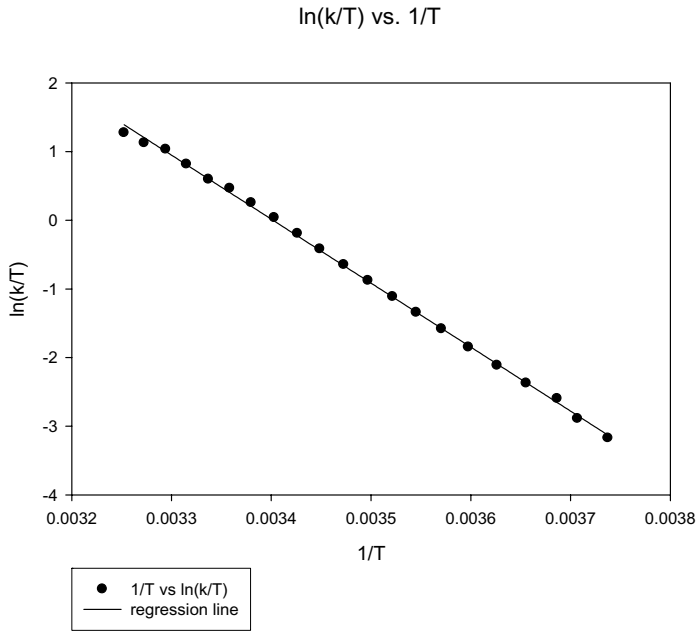

Figure 4. Plot of ln(k/T) vs. 1/T(K) for acetonitrile exchange in complex **2**. Figure reproduced with permission from reference (9). Copyright 2006, American Chemical Society.

X-Ray Crystallography. The tungsten hydrazido complexes **4-6** were prepared to provide an alternative to addition of hydrazine derivatives into the carrier gas during deposition of metal nitride films, a process that has been reported to lower the deposition temperature of TiN films (25-27). Further support for this strategy came from the report that hydrazido complexes were viable single-source precursors for the deposition of TiN thin films while maintaining the positive effects of hydrazine as a co-reactant (28). The observation that the apparent activation energy for deposition of WN_xC_y depended on the N(imido)-C bond dissociation energy raised an interesting question about the hydrazido complexes, for which there are two limiting resonance structures (Figure 5). The bond lengths obtained for **4-6** by single crystal X-ray crystallography were consistent with structure A being the major resonance contributor (13, 29). Although the solid state

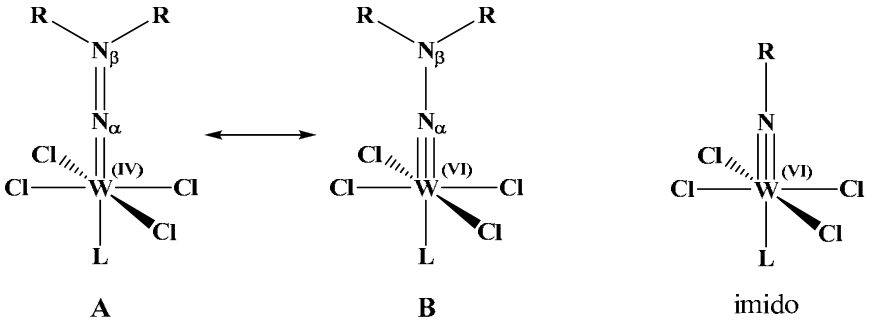

Figure 5. Limiting resonance structures **A** and **B** for hydrazido(2-) complexes of W(VI) and structure of the analogous imido complexes.

structures of **4-6** suggest partial double bonding character between the two nitrogens, **4-6** are viable precursors for the deposition of WN_xC_y, with deposition possible at temperatures as low as 300 °C (14, 30).

TABLE 2. W-N bond distances (Å) for **4-6** and N content of the resulting WN_xC_y films.

Compound	W-N	atom % N in film[a]	reference (W-N)	reference (%N)
4	1.769(5)	24	(13)	(14)
6	1.752(3)	18	(29)	(30)
5	1.742(4)	14	(13)	(30)

[a]Data are the maximum value for WN_xC_y films deposited 350-400 °C

The compositions of WN_xC_y films grown from **4**-**6** show an interesting correlation to the W-N bond lengths (Table 2) and by inference, the relative contributions of the minor resonance structure B to bonding. Complex **5**, in which the N_β lone pair is also conjugated into one of the phenyl rings, shows the shortest W-N bond (largest contribution of limiting structure B) because the N_β lone pair is less available for the N-N multiple bonding seen in limiting structure A. By examination of the structural data, the W-N bond strengths increase **4** → **6** → **5**, but the N content of the film decreases concomitantly.

These results provide a contrast to the behavior of imido complexes **1-3**, for which strong W-N bonding and weak N-C bonding in the imido moiety are associated with higher N contents in the films (12). In films grown from hydrazido complexes **4-6**, a greater contribution of N-N multiple bonding (limiting structure **A**) hinders N-N cleavage. For the hydrazido complexes, this stronger N-N bonding can facilitate pathways that result in incorporation of both N atoms into the film instead of release of one nitrogen through N-N cleavage. Thus the weaker N-N bond of **5** (more B character) may cleave more readily than that of **4**. This N-N cleavage would release one of the nitrogens as an NPh_2 fragment. For complex **4**, the greater extent of multiple bonding in the $W\text{-}N_\alpha\text{-}N_\beta$ moiety (more A character) would minimize N-N cleavage and facilitate other pathways in which the intact hydrazido ligand is incorporated into the film, raising the N content. This interpretation is also consistent with the positive ion CI mass spectra of **4** and **5**, in which no fragments corresponding to N-N cleavage are found in the MS of **4** while the base peak of **5** is $[Ph_2NH_2]^+$, a product of dissociation of the N-N bond (29).

Computational Results

Unprecedented Reaction Pathways. Although prediction of decomposition mechanisms using well-precedented solution chemistry can be quite successful, the higher temperature and different conditions (gas phase and gas-solid reactions) encountered in CVD can result in new reaction pathways that have not been reported for solution phase chemistry. An interesting example can be seen in the CVD of WN_xC_y films from **1-3** in the presence of H_2 carrier gas. In these cases, no chlorine could be detected in the resulting films. RGA (Residual Gas Analyzer) data indicated the presence of HCl (but not Cl_2 or alkyl/aryl chlorides) in the reactor effluent, suggesting involvement of the H_2 carrier gas in removing the chloride ligands from the precursors. Since known reaction pathways of metal chlorides in the presence of H_2 would not lead to HCl, a DFT computational study was undertaken (9).

Assuming that the dissociative loss of CH_3CN from **1-3** under CVD conditions would be rapid (*vide supra*), we examined possible reactions of the coordinatively unsaturated complexes $WCl_4(NR)$ [**1a**: R = Ph; **2a**: R = ^{i}Pr; **3a**: R = allyl] with H_2 in the gas phase to model reactions occurring in the heated zone above the substrate surface. Oxidative addition of H_2 is not possible due to the d^0 electron count of **1a-3a** and as expected, local minima associated with formation of the dihydride could not be found. Although precoordination of H_2 as a σ-complex has been reported to lie in a shallow well in prior DFT studies of electron poor d^0 species (31), we could not locate such a minimum for approach of H_2 to **1a-3a** in preparation for proton transfer to chloride from an acidic H_2 ligand. We then explored pathways for σ-bond metathesis, in which ligand exchange occurs via a 4-center transition state. Such pathways are common for the reaction of d^0 metal alkyls with H_2, but have not been reported for the reaction of metal chlorides with H_2 in solution under standard laboratory conditions. However, we could computationally locate transition states for σ-bond metathesis of **1c-3c** with H_2 to generate the metal hydride products $WCl_3H(NR)$ (**1b-3b**) and HCl. Although the reactions are endothermic with calculated activation energies of approximately 37 kcal/mol, under the high temperature (450 to 750 ^oC) and H_2 flux in the CVD reactor, σ-bond metathesis appears to be a viable route to the experimentally observed chloride-free films and HCl byproduct, providing an example of an unexpected reaction that becomes accessible during CVD.

Gas Phase Variants of Solution Reactions. The observation that addition of NH_3 during film deposition from **2-4** and **6** resulted in higher N content in the resulting films (20, 30, 32, 33), led us to carry out a DFT computational study of the reactions of **2** and **3** with NH_3 (18). Loss of CH_3CN was once again assumed to be rapid under CVD conditions and calculations began with the coordinatively unsaturated species $WCl_4(NR)$ (**2a** and **3a**). Exothermic coordination of NH_3 to the empty coordination site of **2a** (Figure 6a) was followed by conversion to the bis-amide complex **TI-2**. A second proton transfer completed the transamination process to afford the parent imido complex $Cl_4W{=}NH$ and isopropylamine. Comparison of the energetics in Figure 6a with calculated results for unimolecular reactions of **2a** suggests that transamination will be the dominant reaction of the imido moiety in the presence of NH_3, consistent with calculations previously reported for the reaction of NH_3 with $(^tBuN)_2W(NH^tBu)_2$ under ALD conditions (34) and the observation of transamination reactions of imido compounds in solution (35-37).

Computational results also elucidate an additional pathway for removal of the chloride ligands of **1-6** as HCl. In the presence of H_2 carrier gas, the W-Cl bonds were cleaved by σ-bond metathesis. When NH_3 is added to the system, the chlorides could also be removed either in the gas phase by addition of NH_3 followed by elimination of HCl (38-40) or via surface reaction with species generated from NH_3 (41, 42). Calculations on elimination of HCl from the NH_3 adduct **TI-1** reveal a low energy pathway that results in formation of the amido complex **EI-1** (Figure 6b). These pathways not only provide routes for loss of chloride during deposition, they also afford intermediates with additional N-bound ligands in the coordination sphere, facilitating incorporation of higher levels of N in the resulting films as experimentally observed for depositions in the presence of NH_3.

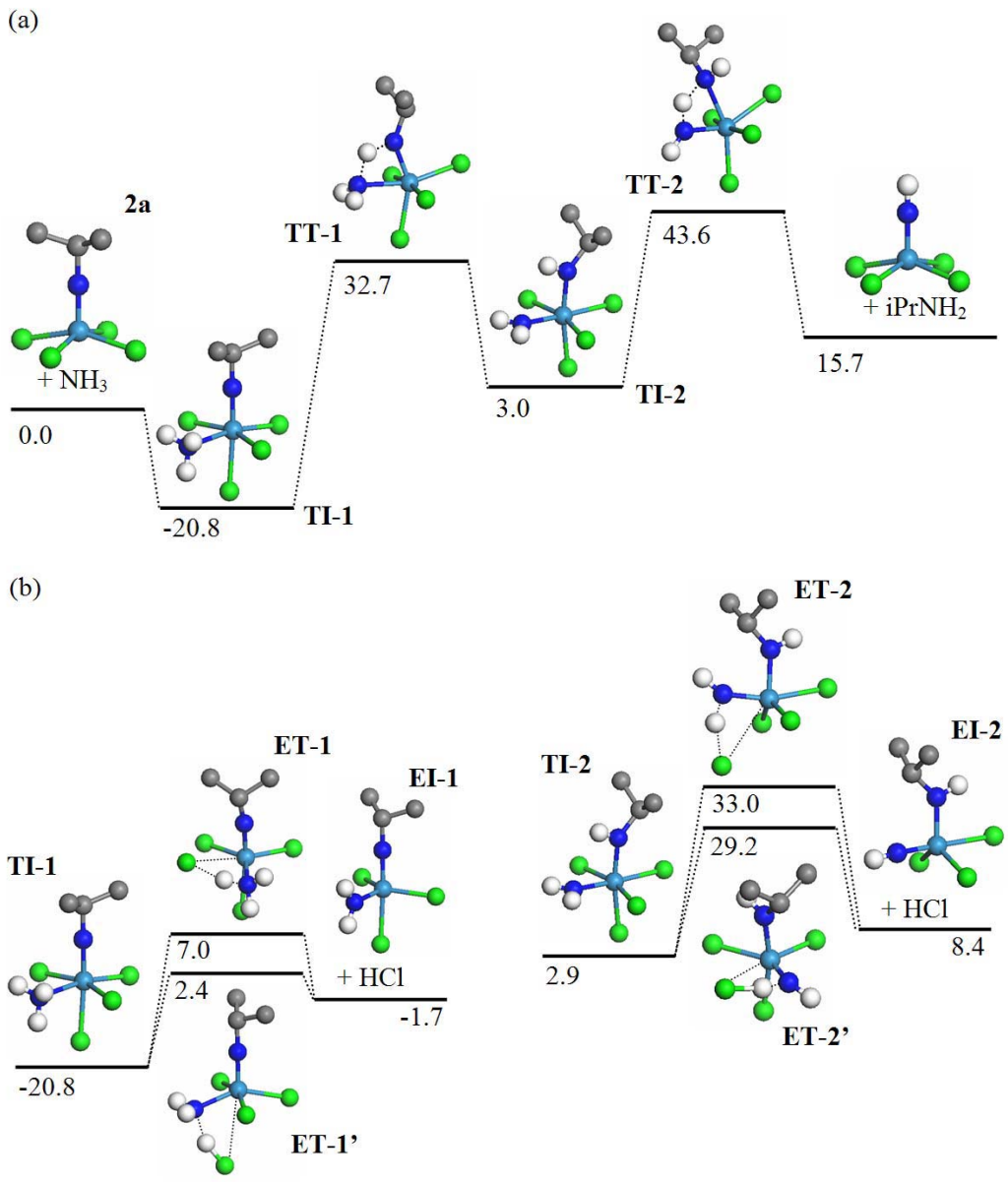

Figure 6. Energetics for (a) transamination of **2a** with NH_3 and (b) 1,2-elimination of HCl from **TI-1** and **TI-2**. Enthalpy values (ΔH°_{298}) are reported in kcal/mol. Hydrogens on the isopropyl groups are omitted for clarity. Figure reproduced with permission from reference (18). Copyright 2008, American Chemical Society.

Summary

Design of organometallic CVD precursors can utilize data obtained from several standard spectroscopic, computational and structural techniques to provide insight into possible decomposition pathways during deposition of thin films. Although care must be taken in extrapolating results obtained under typical laboratory conditions to the temperatures and heterogeneous reactions found in CVD, it is still possible to correlate predicted reaction pathways to film properties. Continued work along these lines will

surely result in increasing sophistication of precursor designs and improved control over film composition and microstructure.

Acknowledgments

Our work on CVD precursors has been generously supported over the years by the Army Research Office, the Office of Naval Research and the National Science Foundation.

References

1. C. H. Winter, W. Zheng and H. M. El-Kaderi, in *Encyclopedia of Inorganic Chemistry* (Wiley, Chichester, 2005), Vol. 5, p. 3121.
2. L. McElwee-White, *Dalton Trans.*, 5327 (2006).
3. A. C. Jones, H. C. Aspinall and P. R. Chalker, *Surf. Coat. Technol.* **201**, 9046 (2007).
4. A. C. Jones, *J. Mater. Chem.* **12**, 2576 (2002).
5. L. G. Hubert-Pfalzgraf, *J. Mater. Chem.* **14**, 3113 (2004).
6. O. Just, B. Obi-Johnson, J. Matthews, D. Levermore, T. Jones and W. S. Rees, Jr., *Mater. Res. Soc. Symp. Proc.* **606**, 3 (2000).
7. C. H. Winter, *Aldrichimica Acta* **33**, 3 (2000).
8. B. D. Fahlman, *Current Organic Chemistry* **10**, 1021 (2006).
9. Y. S. Won, Y. S. Kim, T. J. Anderson, L. L. Reitfort, I. Ghiviriga and L. McElwee-White, *J. Am. Chem. Soc.* **128**, 13781 (2006).
10. O. J. Bchir, K. M. Green, M. S. Hlad, T. J. Anderson, B. C. Brooks, C. B. Wilder, D. H. Powell and L. McElwee-White, *J. Organomet. Chem.* **684**, 338 (2003).
11. O. J. Bchir, S. W. Johnston, A. C. Cuadra, T. J. Anderson, C. G. Ortiz, B. C. Brooks, D. H. Powell and L. McElwee-White, *J. Cryst. Growth* **249**, 262 (2003).
12. O. J. Bchir, K. M. Green, H. M. Ajmera, E. A. Zapp, T. J. Anderson, B. C. Brooks, L. L. Reitfort, D. H. Powell, K. A. Abboud and L. McElwee-White, *J. Am. Chem. Soc.* **127**, 7825 (2005).
13. J. Koller, H. M. Ajmera, K. A. Abboud, T. J. Anderson and L. McElwee-White, *Inorg. Chem.* **47**, 4457 (2008).
14. H. M. Ajmera, T. J. Anderson, J. Koller, L. McElwee-White and D. P. Norton, *Thin Solid Films*, DOI:10.1016/j.tsf.2009.1004.1036 (2009).
15. C. H. Winter, K. C. Jayaratne and J. W. Proscia, *Mater. Res. Soc. Symp. Proc* **327**, 103 (1994).
16. C. J. Carmalt, A. C. Newport, I. P. Parkin, A. J. P. White and D. J. Williams, *J. Chem. Soc. Dalton Trans.*, 4055 (2002).
17. C. J. Carmalt, A. Newport, I. P. Parkin, P. Mountford, A. J. Sealey and S. R. Dubberley, *J. Mater. Chem.* **13**, 84 (2003).
18. Y. S. Won, Y. S. Kim, T. J. Anderson and L. McElwee-White, *Chem. Mater.* **20**, 7246 (2008).
19. O. J. Bchir, T. J. Anderson, B. C. Brooks and L. McElwee-White, in *Chemical Vapor Deposition: CVD XVI (16th)*, edited by M. Allendorf, F. Maury and F. Teyssandier (Electrochemical Society, Pennington NJ, 2003), Vol. 2003-08, p. 424.

20. O. J. Bchir, K. C. Kim, T. J. Anderson, V. Craciun, B. C. Brooks and L. McElwee-White, *J. Electrochem. Soc.* **151**, G697 (2004).
21. C. C. Amato, J. B. Hudson and L. V. Interrante, *Mater. Res. Soc. Symp. Proc.* **168**, 119 (1990).
22. T. S. Lewkebandara, P. H. Sheridan, M. J. Heeg, A. L. Rheingold and C. H. Winter, *Inorg. Chem.* **33**, 5879 (1994).
23. S. W. Benson, *Thermochemical Kinetics*, 2nd ed. (Wiley-Interscience, New York, 1976).
24. G. Hogarth and I. Richards, *Dalton Trans.*, 760 (2005).
25. D. A. Wierda and C. Amato-Wierda, *Proc. Electrochem. Soc.* **2000-13**, 497 (2000).
26. C. Amato-Wierda and D. A. Wierda, *J. Mater. Res.* **15**, 2414 (2000).
27. C. Amato-Wierda, E. T. Norton, Jr. and D. A. Wierda, *Mat. Res. Soc., Symp. Proc.* **606**, 91 (2000).
28. J. T. Scheper, P. J. McKarns, T. S. Lewkebandara and C. H. Winter, *Mater. Sci. Semicond. Process* **2**, 149 (1999).
29. J. Koller, Ph.D. dissertation, University of Florida (2008).
30. D. Kim, O. H. Kim, T. J. Anderson, J. Koller and L. McElwee-White, unpublished results.
31. E. Folga and T. Ziegler, *Can. J. Chem.* **70**, 333 (1992).
32. H. M. Ajmera, A. T. Heitsch, O. J. Bchir, T. J. Anderson, L. L. Reitfort and L. McElwee-White, *J. Electrochem. Soc.* **155**, H829 (2008).
33. D. Kim, O. H. Kim, T. J. Anderson, J. Koller, L. McElwee-White, L. C. Leu, J. M. Tsai and D. P. Norton, *J. Vac. Sci. Technol. A*, DOI: 10.1116/1111.3106625 (2009).
34. A. B. Mukhopadhyay and C. B. Musgrave, *Appl. Phys. Lett.* **90**, 173120 (2007).
35. M. P. Coles, C. I. Dalby, V. C. Gibson, W. Clegg and M. R. J. Elsegood, *Polyhedron* **14**, 2455 (1995).
36. A. J. Blake, P. E. Collier, S. C. Dunn, W.-S. Li, P. Mountford and O. V. Shishkin, *J. Chem. Soc., Dalton Trans.*, 1549 (1997).
37. H.-T. Chiu, S.-H. Chuang, G.-H. Lee and S.-M. Peng, *Polyhedron* **13**, 2443 (1994).
38. M. Siodmiak, G. Frenking and A. Korkin, *J. Mol. Model.* **6**, 413 (2000).
39. J. B. Cross and H. B. Schlegel, *Chem. Mater.* **12**, 2466 (2000).
40. A. G. Baboul and H. B. Schlegel, *J. Phys. Chem. B* **102**, 5152 (1998).
41. Y. Widjaja and C. B. Musgrave, *Surf. Sci.* **469**, 9 (2000).
42. H. Tiznado, M. Bournan, B. C. Kang, K. Lee and F. Zaera, *J. Mol. Catal. A: Chem.* **281**, 35 (2008).